Phys. Lett. B 850 (2024) 138470

Contents lists available at ScienceDirect

Physics Letters B

journal homepage: www.elsevier.com/locate/physletb

Letter

Neutron capture reaction cross-section of ^{79}Se through the ^{79}Se(d,p) reaction in inverse kinematics

N. Imai [a,*], M. Dozono [a,1], S. Michimasa [a], T. Sumikama [c], S. Ota [a,2], S. Hayakawa [a], J.W. Hwang [a,b], K. Iribe [d], C. Iwamoto [a], S. Kawase [e], K. Kawata [a], N. Kitamura [a], S. Masuoka [a], K. Nakano [e], P. Schrock [a], D. Suzuki [c], R. Tsunoda [a], K. Wimmer [f,3], D.S. Ahn [c,b], O. Beliuskina [a,4], N. Chiga [c], N. Fukuda [c], E. Ideguchi [h], K. Kusaka [c], H. Miki [i], H. Miyatake [g], D. Nagae [c], S. Ohmika [j], M. Ohtake [c], H.J. Ong [h], H. Otsu [c], H. Sakurai [c], H. Shimizu [a], Y. Shimizu [c], X. Sun [c], H. Suzuki [c], M. Takaki [a], H. Takeda [c], S. Takeuchi [i], T. Teranishi [d], Y. Watanabe [e], Y.X. Watanabe [g], K. Yako [a], H. Yamada [i], H. Yamaguchi [a], L. Yang [a], R. Yanagihara [h], Y. Yanagisawa [c], K. Yoshida [c], S. Shimoura [a]

[a] Center for Nuclear Study, the University of Tokyo, Hirosawa 2-1, Wako, 351-0198, Saitama, Japan
[b] Center for Exotic Nuclear Studies, Institute of Basic Science, Expo-ro 55, Yuseong-gu, 34126, Daejeon Republic of Korea
[c] RIKEN Nishina Center, Hirosawa 2-1, Wako, 351-0198, Saitama, Japan
[d] Department of Physics, Kyushu University, Motooka 744, Nishi, Fukuoka, 819-0395, Fukuoka, Japan
[e] Department of Advanced Energy Engineering Science, Kyushu University, 6-1 Kasuga-koen, Kasuga, 819-8580, Fukuoka, Japan
[f] University of Tokyo, Hongo 7-3-1, Bunkyo, 113-0033, Tokyo, Japan
[g] KEK Wako Nuclear Science Center, Hirosawa 2-1, Wako, 351-0198, Saitama, Japan
[h] Research Center for Nuclear Physics, Osaka University, 10-1 Mihogaoka, Ibaraki, 567-0047, Osaka, Japan
[i] Deparment of Physics, Tokyo Institute of Technology, 2-12-1 Ookayama, Meguro, 152-8550, Tokyo, Japan
[j] Deparment of Physics, Saitama University, Shimo-Okubo 255, Sakura-ku, Saitama, 338-8570, Saitama, Japan

ARTICLE INFO

Editor: Betram Blank

ABSTRACT

γ emission probabilities from unbound states in ^{78,80}Se, populated by a neutron-transfer reaction (d,p) on ^{77,79}Se nuclei in inverse kinematics, were measured by directly detecting reaction residues. Assuming the spin distribution at the respective excitation energy of the unbound state, the cross-sections of the ^{79}Se$(n,\gamma)^{80}$Se reaction were evaluated using the γ emission probabilities. The surrogate-ratio method with the experimental γ emission probabilities of ^{78,80}Se was also employed to deduce the cross-sections of ^{79}Se(n,γ) reaction by incorporating the theoretical evaluations of the neutron-capture reaction on the isomeric state in ^{77}Se. Our two cross-sections are in good agreement with existing nuclear data compilations for the neutron-capture reaction on ^{79}Se. The presented method contributes to the body of existing knowledge by providing approaches for determining the neutron capture cross-sections of radioactive nuclei at various neutron energies.

Neutron-induced reactions of long-lived isotopes are envisaged for the transmutation of nuclear waste from nuclear power plants. In most countries, highly radioactive waste left over after the reprocessing of spent uranium fuel will is stored in an underground repository, where it will remain for longer than 10^6 years due to the long lifetimes of these radioactive isotopes. One way of handling such long-lived fission products is to neutralize waste through nuclear reactions [1–4]. Decommissioning nuclear waste by employing high flux accelerators [1,4] and

* Corresponding author.
E-mail address: n.imai@cns.s.u-tokyo.ac.jp (N. Imai).
[1] Present address: Department of Physics, Kyoto University, Japan.
[2] Present address: RCNP, Osaka University, Japan.
[3] Present address: GSI, Germany.
[4] Present address: Department of Physics, University of Jyväskyla, Finland.

https://doi.org/10.1016/j.physletb.2024.138470
Received 12 June 2022; Received in revised form 17 October 2023; Accepted 15 January 2024
Available online 18 January 2024

fast reactors [2,3] has been proposed. However, to design such facilities, reaction cross-sections in a wide energy range are indispensable.

The neutron capture reaction is also related to the search for the origin of matter in the universe. Elements heavier than iron are produced by successive neutron capture reactions (n,γ) and β^- decays [5]. By comparing the observed abundance distribution of elements with nucleosynthesis calculations employing (n,γ) cross-sections and β^- decay properties, both the neutron-density and temperature of an astrophysical site may be constrained, thereby microscopically probing the origin of the elements.

^{79}Se is placed in the reaction path of the s-process. Although ^{79}Se is radioactive, its half-life is up to 3.2×10^5 years, therefore, the main nucleosynthesis path proceeds to ^{80}Se by neutron capture. However, because ^{79}Se has a low-lying isomeric state at 95.8 keV, which can directly β^- decay to ^{79}Br, an alternative path can open depending on the temperature of the astrophysical site, which makes ^{79}Se a stellar thermometer [6]. To determine the properties of the thermometer, the measurement of the neutron capture reaction on ^{79}Se is needed.

The neutron capture reaction can be generally categorized into two processes: direct radiative capture reaction, and compound nuclear (CN) reaction. The cross-section of the first reaction is described by the final state wave function, which can be determined by a transfer reaction, such as the (*d, p*) reaction [7]. For the CN reaction, since a large number of levels above the particle-emission threshold are involved, (i.e., approximately 10 MeV in ^{80}Se), the number is estimated to be as high as 7×10^4 MeV^{-1}, and the cross-sections are usually expressed by a statistical model [8].

The (n,γ) cross-section in the CN reaction can be described as the product of two parts: the formation of the excited state and the subsequent γ emission to lower bound states which is referred to as a γ-emission channel. The formation cross-section of a CN can be calculated using optical model potentials [8]. However, it is difficult to theoretically estimate the survival probability, in which the CN releases its internal energy by emitting γ rays instead of particles. Indirect methods to determine CN reaction cross-sections have been studied extensively [9–11].

The theoretical gamma emission probability, P_γ, is determined by the competition of gamma emissions against particle emissions. P_γ is considered to depend on both the total spin of the state and the excitation energy, E_x. Although the distributions of the spin and parity of the unbound states populated by CN reactions may differ from those of transfer reactions, the P_γ of the populated state can be considered identical. The P_γ can be obtained from the transfer reaction by considering the spin parity distributions of the reactions. In fact, in the absolute surrogate reaction techniques, spin-dependent P_γ has been deduced by measuring the multi-polarities of subsequent γ decays using a statistical model [9].

When the kinetic energy dissipated in a deuteron-induced reaction increases, the dominant reaction process gradually changes from a pre-equilibrium to a compound reaction [12]. In the pre-equilibrium reaction, some internal collisions are involved in the nucleus. Since the angular momenta of particles and holes excited in the reaction are coupled with the initial spin and transferred angular momentum, the spin-parity distribution can be close to the statistical distribution by the compound process, which is adopted by the TALYS-1.9 [13]. However, to explain the reaction mechanism required to populate the unbound states by the transfer reactions, theoretical works in the framework of the direct reactions [14,15] concluded that the larger angular momenta were transferred to the state than the case of the neutron-capture reaction and that the transferred angular momentum depends on the nuclear structure.

In the current work, the P_γ of the unbound ^{80}Se state was determined to evaluate the neutron capture cross-sections of ^{79}Se by directly identifying the residual nuclei. The nuclear reaction using inverse kinematics rendered measurement with this technique feasible. The long half-life of ^{79}Se makes it one of the longest-lived fission products of highly radioactive nuclear waste. However, to date, the (n,γ) cross-section has never been measured directly. This is partly due to the difficulty of creating an enriched sample of ^{79}Se [16]. However, the cross-section has been studied indirectly using the dipole strength distribution deduced through ^{80}Se(γ,γ') [17]. The experimental technique utilizes a real photon to deduce the dipole strength. The presented method, used to determine P_γ experimentally, provides an alternative way to evaluate the (n,γ) cross-sections on the radioactive nuclei.

Table 1
Properties of the ground and isomeric states of ^{77,79}Se.

	^{77}Se		^{79}Se	
E_x (keV)	0.0	161.9	0.0	95.8
J^π	$1/2^-$	$7/2^+$	$7/2^+$	$1/2^-$
half-life	stable	17.4 s	3.26×10^5 y	3.92 m

In addition to determining P_γ, the surrogate-ratio method was used to deduce the (n,γ) cross-sections of ^{79}Se. A problem related to the surrogate reaction lies in the spin distribution of the (n,γ) reaction, which may differ from the surrogate reaction. To overcome this, the surrogate-ratio method was employed, which is less dependent on the angular momentum difference [18,19]. Within the framework of the surrogate-ratio method, the desired (n,γ) cross-section can be written as follows:

$$\sigma^{(n,\gamma)}_{^{79}\mathrm{Se}}(E)=\sigma^{(n,\gamma)}_{^{77}\mathrm{Se}}(E)\times\frac{\sigma^{CN}(^{80}\mathrm{Se})}{\sigma^{CN}(^{78}\mathrm{Se})}\times\frac{P_\gamma^{^{80}\mathrm{Se}}(E)}{P_\gamma^{^{78}\mathrm{Se}}(E)}. \quad (1)$$

Here, $\sigma^{(n,\gamma)}_{^{79}\mathrm{Se}}$ and $\sigma^{CN}(^{80}\mathrm{Se})$ are the (n,γ) cross-section and the formation cross-sections of the CN state, respectively. The latter was calculated using TALYS-1.9 [13] code and the Jeukenne-Lejeune-Mahaux optical potential [20]. In the current study, $P_\gamma^{^{80}Se}(E)$ was determined as the experimental γ-emission probability of ^{80}Se.

Two surrogate reactions, ^{77}Se$(d,p)^{78}$Se and ^{79}Se$(d,p)^{80}$Se, were separately measured under identical experimental conditions carried out at the RI Beam Factory operated by the RIKEN Nishina Center and the Center for Nuclear Studies (CNS), University of Tokyo, by employing the novel "optimized energy degrading optics" (OEDO) for radioactive isotope (RI) beams [21]. The optics were realized by installing two superconducting quadrupole magnets and a high-frequency electric field radio-frequency deflector (RFD). Beam ions, which were generated by the fission reaction of ^{238}U beam with a beryllium target of 1 mm thickness, were identified by the time-of-flight (TOF) between the third (F3) and the fifth (F5) focal planes of the BigRIPS separator [22] measured by diamond detectors [23]. For the ^{79}Se beam, the measured purity was 40% and the main contaminants were ^{80}Br and ^{78}As. However, the TOF indicated that they were well separated by 7 σ from ^{79}Se. The beam energy was degraded at F5 using a 3.5-mm-thick Al degrader, resulting in a beam energy of 26 MeV/nucleon. Both ^{77,79}Se nuclei have low-lying isomeric states, as shown in Table 1 and the neutron separation energies S_n of ^{78,80}Se are 10.497 and 9.913 MeV, respectively. The isomer ratio was measured to be 87 ± 7% in ^{77}Se beams. On the other hand, for ^{79}Se the ratio was measured to be 29 ± 7% in the past experiment at RIBF with the same primary beam of ^{238}U and the Be target [24]. Considering that the fission reaction produces the high excited states, the isomer ratio can be considered as a result of the number of the magnetic substates of $7/2^+$ and $1/2^-$. Namely, the $7/2^+$ state was around 80% in both the beams. Hereafter, to clarify that the beam included both the isomeric and ground states, the states are referred to as Se_{iso} and $\mathrm{Se}_{g.s.}$, respectively. When both states are mixed, it is denoted as Se_{mixed}.

Even though the isomeric state is included in the beam, the calculated spin distribution suggests that the influence of the $1/2^-$ state on the P_γ is expected to be small. First, the spin distributions were calculated using TALYS-1.9, specifically at the excitation energy of 10 MeV, which is around S_n in ^{78,80}Se after the transfer reaction on both the ground and isomeric states of ^{77,79}Se, respectively. The distributions

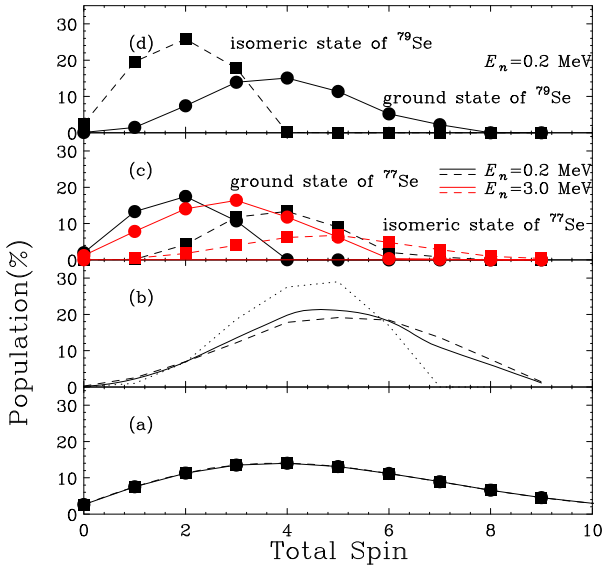

Fig. 1. Calculated total spin distributions for the different reactions, (a) Distribution in ^{80}Se by (d,p) reactions at 20 MeV/nucleon on both the ground (solid line) and isomeric states (dashed line) in ^{79}Se by TALYS-1.9. Although it is not shown here, there are strength of 4% at $J > 9$. (b) Distributions estimated by the DWBA calculation with several angular momentum transfers to ^{80}Se by (d,p) reaction from the ground $7/2^+$ state (dashed line) and the isomeric $1/2^-$ state (dotted line) of ^{79}Se, respectively. The solid line is the expected distribution of 80% $7/2^+$ and 20% $1/2^-$. (c) The black solid line is the calculated distribution with the neutron capture of $E_n = 0.2$ MeV with a ground state of ^{77}Se, while the dashed line is the population with the isomeric state of ^{77}Se. The red line is the case of $E_n = 3.0$ MeV (d) Same as for the neutron capture reactions of $E_n = 0.2$ MeV with ^{79}Se. The black solid line is for the case of the ground state in ^{77}Se, while the dashed line is for the isomeric state.

were found to be almost identical for both the ground and isomeric states, as presented in Fig. 1(a). In TALYS-1.9, the total spin distribution is assumed to be the same as for the fusion reaction, where the equilibrium inside the nucleus is realized so that the spin-distribution will be close to the distribution of the level density.

As for the other extreme cases, the direct reaction of the (d,p) reaction to populate the excited state at 10 MeV was studied. The cross-sections of the angular momentum transfer of $\Delta L = 0 - 5$ were calculated using the DWBA code DWUCK5 [25] with the bound state approximation, where the form factor was assumed to be a single particle wave function with a binding energy of 100 keV. The spectroscopic factors were assumed to be one unit for all cases. The final spin strength distribution was obtained by accounting for three factors: the coupling between the transferred spin and the target-spin, the calculated cross-sections and the spin-dependent level density at 10 MeV of ^{80}Se, which was deduced using the Back-shifted Fermi-gas model. The solid (dashed) lines in Fig. 1(b) are the populated spins from the ground (isomeric) state of ^{79}Se. The distributions are similar to each other and they center around $J \simeq 5$, similar to those calculated by TALYS-1.9, suggesting that the distribution is mainly governed by the level density distribution. When the spin-dependent γ emission probabilities are taken into account, the P_γ are 39% and 32%, respectively, for the distribution by TALYS-1.9 in Fig. 1(a), and the DWBA calculation with 80% of the $7/2^+$ state and 20% of the $1/2^-$ state. The actual distribution may be the middle of (a) and (b); therefore the effect of the target-spin difference can be expected to be smaller than 18%.

The RFD selected almost only the beam of ^{77}Se$_{mixed}$ or ^{79}Se$_{mixed}$ from the cocktail beam, and it reduced the beam spot size at the secondary target, a 4 mg/cm^2-thick CD_2 foil. A pair of parallel plate avalanche counters (PPACs) were placed 10.4 m downstream from the RFD, which provided timing information and the emittance of the beam of ^{77}Se$_{mixed}$ or ^{79}Se$_{mixed}$ on the target. The beam intensities of the Se beams were approximately 15 kHz, which was limited by the total beam rate of around 700 kHz at F3. The target, placed 1.4 m downstream of the PPACs, was bombarded by the beam to induce a one-neutron transfer reaction Data were collected for 1 days for each beam.

The incident beam energy on the target was measured as 20 ± 1 MeV/nucleon, where the error stands for 1σ of the distribution. The energy on the target for each ion was determined event-by-event by measuring the TOF of 14.8 m, which allowed us to determine the energy with 0.3% accuracy. This gives rise to an energy resolution of approximately 20 keV in the center of mass (c.m.) frame. The uncertainty of the beam energy is negligibly small.

The recoiled particles from the CD_2 target were measured using a silicon strip detector (SSD)-CsI(Tl) array TiNA, an array comprising six telescopes, each having an SSD (Micron semiconductor Ltd.) type YY1 and two CsI(Tl) crystals. The telescopes were placed roughly 8 cm upstream of the target in a lampshade-like, fully covering the azimuthal angles. The array covered 100° to 150° of the polar angles in the laboratory frame, which corresponded to 9° to 34° in the c.m. frame for the excited states of 10 MeV. The excitation energies of the states populated in ^{78,80}Se were determined from the measured momenta of the protons and the incident beam. By taking into account the uncertainty of the reaction point in the target and the size of the YY1 strip, the energy resolution in the c.m. frame was estimated to be 0.8 (1.3) MeV (σ) at the excitation energy of 10 (13) MeV.

Since the reaction occurred under inverse kinematics, the beam-like products moved in the forward angles. The momentum of the outgoing residual nuclei was analyzed by a part of the SHARAQ spectrometer [26], comprising two quadrupole magnets and a dipole magnet. The total momentum acceptance of the spectrometer was 6%. A pair of PPACs and an ionization chamber (IC) were placed at the focal plane of the spectrometer, which was roughly 7 m downstream of the secondary target. The charge-to-mass ratio, A/Q, of the outgoing residual nucleus was determined from the magnetic rigidity and the velocity between the secondary target and the PPACs. The trajectory of the ions measured by PPACs was used to determine the flight length inside the spectrometer. The IC was 28 cm wide, 15 cm high, and had a 75.7 cm depth, and it had 30 rectangular electrodes in the longitudinal direction to measure the Bragg curve of the beams. The IC was filled with 100 Torr carbon tetra fluoride gas, which provided a fast electron velocity of 6 cm/ μs. The velocity enabled us to measure the curves, even though the unreacted beam also entered the IC. Prior to the low energy measurement, the relative gain was adjusted by injecting the fast ^{79}Se$_{mixed}$ beam into the IC, where the energy loss in each electrode was calculated to be close to constant. By selecting the momenta of the ejectiles, the fusion reaction with the carbon in the CD_2 target was rejected. The beam range was obtained by fitting the Bragg curve to the measured energy loss distribution in the IC. The height of the Bragg curve allowed us to determine the atomic numbers of the ejectiles.

Fig. 2(a) presents the correlation between the range, (equivalent to the mass), and A/Q ratio of the reaction products obtained by ^{79}Se$_{mixed}(d,p)$X reaction, for events where the incident ^{79}Se$_{mixed}$ beam and recoiled protons were identified. The loci allowed us to identify outgoing residual nuclei. Here, X is one of the reaction residues of ^{78,79,80}Se. To obtain the A/Q ratio, the first order optical transfer matrix was used. Therefore, at the edge of the focal plane, namely, apart from the central value in A/Q, the A/Q slope were observed to be tilted. The projection to the horizontal axis is shown in Fig. 2(b). Three strong loci were observed at roughly $A/Q = 2.32$, 2.39 and 2.47, respectively, which corresponded to three charge states at 34+, 33+, and 32+ of ^{79}Se, respectively. Because the A/Q resolution was optimized for the central trajectory, the loci away from the center ($A/Q \simeq 2.39$) distributed more widely so that ^{80}Se^{34+} and ^{78}Se^{33+} are overlapped in Fig. 2(b). However, with the range information, these two loci can be separated. ^{80}Se$^{33+,32+}$ isotopes were observed in $2.404 < A/Q < 2.430$, $2.486 < A/Q < 2.520$, respectively. When the residual nucleus was ^{80}Se, no particle was emitted. Therefore, the γ-emission probability was ob-

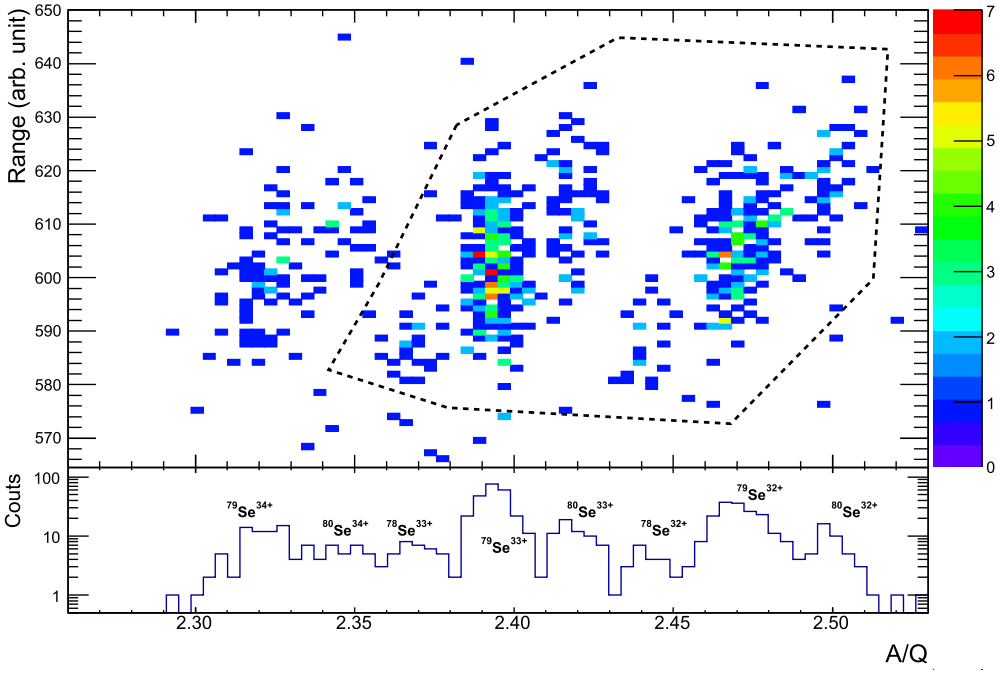

Fig. 2. (a) The ranges of residual nuclei are shown against the A/Q ratio for the ^{79}Se(d,p)X reaction. Here, X represents either of ^{78,79,80}Se. The dashed line is the selected region of $^{78-80}$Se$^{32+,33+}$. (b) A/Q histogram which was obtained by projecting (a) to the X axis. The name of isotope with the respective charge state is shown beside each peak.

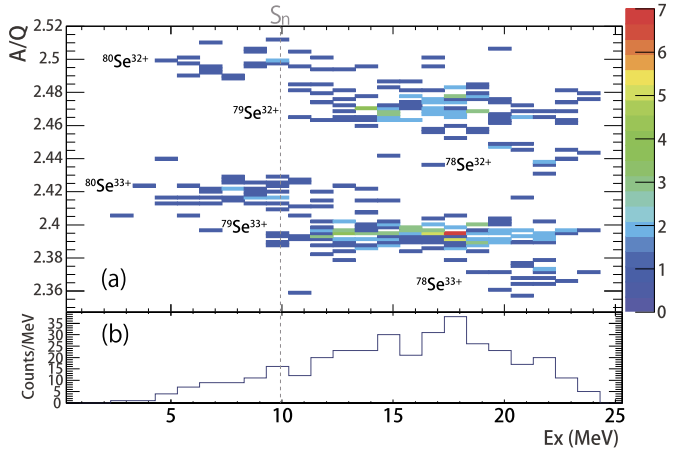

Fig. 3. (a) The charge-to-mass ratio, A/Q, as a function of the E_x of ^{80}Se after selecting the recoiled protons and helium-like 32+, 33+ ions in Fig. 2. (b) Projection of (a) to the excitation energy distribution of ^{80}Se.

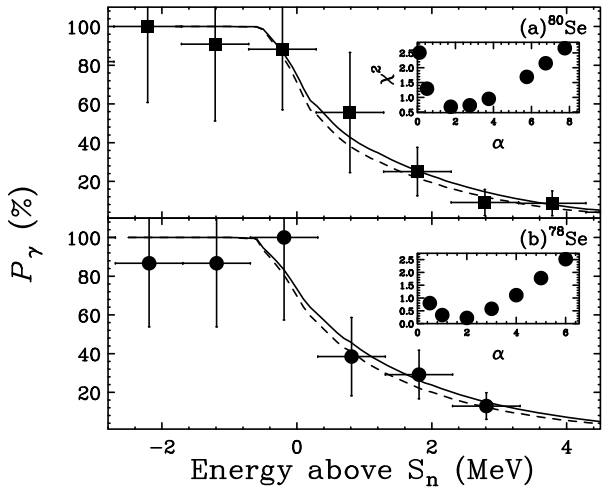

Fig. 4. Experimental P_γ for (a) ^{80}Se and (b) ^{78}Se, respectively, as a function of the excitation energy above S_{1n}. The solid and dashed lines are the γ emission probabilities using different models of the level density [27,28]. The insets of both panels present the χ^2 distributions as a function of α.

tained by taking a ratio of the yield of ^{80}Se ions to the sum of ^{78,79,80}Se at each excitation energy. To measure the outgoing ions, the magnetic rigidity of the spectrometer was set to focus ^{79}Se^{33+} at the horizontal center of the IC. Because the geometrical acceptance of the spectrometer was reduced at the edge of the focal plane, (i.e., some 34+ events were halted in the spectrometer), the events of Q = 32+ and 33+ were used to determine the probability.

Fig. 3 (a) presents the A/Q ratio as a function of E_x determined by the momenta of the incident beams and recoiled protons when the charge states of 33+ and 32+ were selected for the ^{79}Se(d,p)X reaction, as shown in Fig. 2. Six loci, ^{78,79,80}Se, were observed at $A/Q = 2.36, 2.39$ and 2.42 for the charge state of 33+ and at $A/Q = 2.50, 2.42$ and 2.44 for 32+, respectively. ^{80}Se were observed to survive up to an E_x of 13 MeV, which is higher than S_n of 9.9 MeV by 3 MeV. The two-neutron separation energy of ^{80}Se is 16.87 MeV; thus, ^{78}Se were observed at $E_x > 17$ MeV. The positions of ^{78,79}Se validates the missing mass energy spectra. The excitation energy spectrum of ^{80}Se obtained by projecting E_x is shown in Fig. 3(b). The proton yields increased as the excitation energy increased. However, at approximately 18 MeV in E_x, the energy of the recoil proton was below the threshold of around 1 MeV, which led to a drop in yield.

The experimental P_γs for ^{78}Se and ^{80}Se obtained by the (*d, p*) reaction are shown in Figs. 4(a) and (b). Although the statistical error is large, the P_γ for ^{80}Se was observed to be larger than that for ^{78}Se at around 1 MeV. The P_γ values from the excited states after the binary reaction were calculated using TALYS-1.9, where the spin distribution in each excitation energy, and the γ emission probabilities from a given excitation energy and spin were accounted for. In the calculation, the spin-distributions assuming the pre-equilibrium reaction of Fig. 1(a) were adopted. P_γ curves for ^{78,80}Se which include the excitation-energy

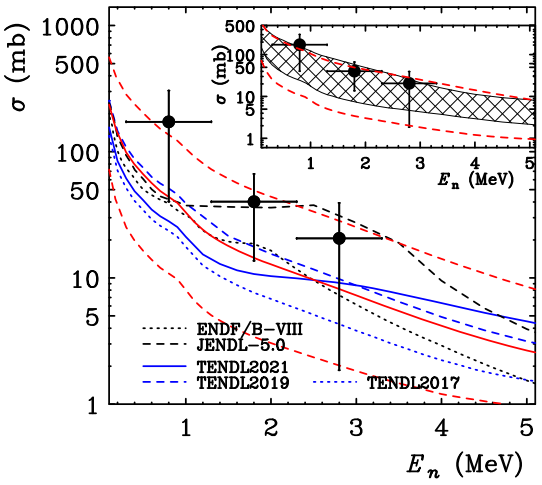

Fig. 5. (n,γ) cross-sections on $^{79}Se_{g.s.}$ with the normalized Γ_γ and the surrogate-ratio method are presented with the statistical errors. The black dotted and dashed lines are the theoretical cross-sections of ENDF/B-VIII and JENDL-5.0, respectively. TENDEL2021, 2019, and 2017 are shown as blue solid, dashed, and dotted lines, respectively. The red solid line indicates the presented calculation with a central value of α, while the red dashed line is the 1σ uncertainty region of α. The data points are the present results of the surrogate-ratio method. The hatched area in the inset represents the cross-sections deduced by the inverse reaction of ^{80}Se(γ,γ') [17].

dependence of the energy resolution are presented in Figs. 4(a) and (b). The solid (dashed) curves are the results with the Constant Temperature + Fermi Gas model [27] (Back-shifted Fermi-gas model [28]) for the level density. The theoretical P_γ curves for both nuclei are reasonably in agreement with the experimental P_γ values.

In the TENDL evaluations, P_γ was modified by changing the normalization factor of the gamma width, Γ_γ. In the evaluation of TENDL2019 [30], the normalization factor for the ^{79}Se(n,γ) reaction, defined here as α, increased to 1.75 from 0.75 of TENDL2017. The α was searched to reproduce the presented P_γ of ^{78}Se using TALYS-1.9. The distribution of χ^2 as a function of α, shown in Fig. 4 (b) inset, indicates that presented result requires $1.6^{+3.5}_{-1.3}$, while $\alpha = 1$ is the recommended value according to TENDL2019, indicating that P_γ deduced from the $^{77}Se_{mixed}(d,p)$ reaction is consistent with the result of the (n,γ) reaction. The same analysis was conducted for the case of P_γ of ^{80}Se, as shown in Fig. 4 (a). The resultant $\alpha = 1.6^{+4.1}_{-1.2}$ was obtained. The mean value is close to the recommended one of TENDL2019.

With the resultant normalization factor of Γ_γ for ^{80}Se, the (n,γ) cross-sections of $^{79}Se_{g.s.}$ were calculated up to 5 MeV above S_{1n} using TALYS-1.9. In the calculation, the other parameters were the same as those used for TENDL2021. As shown in Fig. 5 inset, a comparison of the calculated cross-sections for $^{79}Se_{g.s.}(n,\gamma)^{80}$Se with the cross-sections determined by measuring the photo-absorption of ^{80}Se [17], indicates they agree with each other. A comparison of the (n,γ) cross-sections to three evaluations, ENDF/B-VIII [31], TENDL, and JENDL-5.0 [32], is also made in Fig. 5. Since the uncertainty of α is large, all the theoretical evaluations are placed within the uncertainty of the presented result.

The (n,γ) cross-sections were also evaluated from $E_n = 0.8$ to 4 MeV in 1 MeV steps by employing the surrogate ratio method. Because the ground state spins of ^{77,79}Se are different, the cross-sections of $^{77}Se_{g.s.}(n,\gamma)$ cannot be used as the first term in Eq. (1) to determine the cross-sections of the $^{79}Se_{g.s.}(n,\gamma)$ reaction. In Figs. 1 (c) and (d), calculations of the neutron capture reaction at $E_n = 0.2$ MeV with both the ground state (solid line) and the isomeric state (dashed line) of ^{77,79}Se are presented. The total spin distribution depends on the initial spin of the target nucleus. In (c), the results with $E_n = 0.2, 3$ MeV are presented, indicating as the neutron energy increases, spin-populations with the ground and the isomeric state gets closer to each other, but they are not identical, as in the case of the transfer reactions in (a).

For the surrogate-ratio method to determine $^{79}Se_{g.s}(n,\gamma)$ cross-sections, cross-sections of the neutron-capture reaction on $^{77}Se_{iso}$ is needed. Since the lifetime of the isomeric state is finite, the cross-sections have not been measured; they are calculated using the TALYS-1.9 with the same parameter sets of the Γ_γ for the $^{77}Se_{g.s.}(n,\gamma)$ reaction, for which cross-sections were directly measured at 21, 30, 45, 70 and 510 keV [29]. Since the parameters of the compound states in ^{78}Se are considered to be optimized by the $^{77}Se_{g.s.}(n,\gamma)$ cross-sections, the calculated $^{77}Se_{iso}(n,\gamma)$ reaction cross-section can be expected to be correct. The compound formation cross-section was calculated in a 0.2 MeV neutron-energy step using the TALYS-1.9 code with the parameter set of TENDL2021. The cross-sections using the surrogate-ratio method, plotted in Fig. 5 as points, indicate that the cross-sections are in agreement with our calculation using the $\alpha = 1.6$ for Γ_γ. The deduced cross-sections support TENDL2019 rather than TENDL2017 and TENDL2021 which are lower than the presented results of the surrogate-ratio method.

In summary, we studied the one-neutron transfer reaction on the long-lived radioactive isotope of ^{79}Se in the inverse kinematics at approximately 20 MeV/nucleon. The gamma emission probabilities of the unbound states were directly determined by identifying the reaction residues instead of measuring γ rays. Although the total spin distribution populated by the transfer reaction was calculated to be different from those of the neutron capture reactions around $E_n \simeq 1$ MeV, the normalization factor of Γ_γ determined by the transfer reaction was able to evaluate the neutron capture cross-sections with the theoretical spin distribution. The presented result of the surrogate-ratio method is consistent with TENDL2019, JENDL-5.0 and ENDF/B-VIII.

Obtaining higher statistics for the two surrogate reactions using a thinner target will allow the evaluation of the (n,γ) reactions at $E_n <$ 1 MeV with a finer energy step. By accounting for the long half-life of $^{79}Se_{g.s.}$, once the $^{79}Se_{g.s.}$ beam is provided at Isotope-Separator-On-Line facility like ^{44}Ti [33], the higher beam intensity can be expected, which makes an experiment with the re-accelerated ^{79}Se beam with small statistical uncertainties feasible.

We have demonstrated that a simple and novel experimental technique can determine (n,γ) cross-sections by studying γ emission probability. Studies of neutron capture rates involving long-lived fission products as well as radioactive nuclei located far from the stability line are now feasible, and the results of which can help to design transmutation facilities and reveal the origin of elements in the universe.

Declaration of competing interest

The authors declare that they have no known competing financial interests or personal relationships that could have appeared to influence the work reported in this paper.

Data availability

Data will be made available on request.

Acknowledgements

We would like to thank the RIKEN Nishina Center and the CNS, the University of Tokyo, accelerator staff for their excellent beam delivery. This study was supported by the ImPACT Program of the Council for Science, Technology and Innovation (Cabinet Office, Government of Japan), JSPS KAKENHI Grant Numbers 19H01903 and 19H01914, and the Institute for Basic Science IBS-R031-D1 and IBS-R031-Y2. We are grateful to Prof. Z.G. Xiao, Dr. O. Iwamoto, and Dr. A. Mengoni for their valuable discussions on the presented result. N.I. would like to thank Dr. A. Makinaga for providing their numerical data.

References

[1] OECD/NEA, Accelerator-drive Systems (ADS) and Fast Reactors (FR) in Advanced Nuclear Fuel Cycles, OECD/NEA Report 3109, 2002.
[2] S. Chiba, T. Wakabayashi, Y. Tachi, N. Takaki, A. Terashima, S. Okumura, T. Yoshida, Sci. Rep. 7 (2017) 13961.
[3] T. Wakabayashi, M. Takahashi, S. Chiba, N. Takaki, Y. Tachi, Nucl. Eng. Des. 363 (2020) 110667.
[4] H. Okuno, H. Sakurai, Y. Mori, R. Fujita, M. Kawashima, Proc. Jpn. Acad. Ser. B, Phys. Biol. Sci. 95 (2019) 430.
[5] E.M. Burbudge, G.R. Burbidge, W.A. Fowler, F. Hoyle, Rev. Mod. Phys. 29 (1957) 547–655.
[6] F. Käppler, H. Beer, K. Wisshak, Rep. Prog. Phys. 52 (1989) 945.
[7] K.L. Jones, S.N. Liddick, A.C. Larsen, M. Guttormsen, K. Cooper, A.C. Dombos, D.J. Morrissey, F. Naqvi, G. Perdikakis, S.J. Quinn, T. Renstrøm, J.A. Rodriguez, A. Simon, C.S. Sumithrarachchi, R.G. Zegers, Nature 465 (2010) 454–457.
[8] J.E. Escher, J.T. Harke, F.S. Dietrich, N.D. Scielzo, I.J. Thompson, W. Younes, Rev. Mod. Phys. 84 (2012) 353.
[9] A. Ratkiewicz, et al., Phys. Rev. Lett. 122 (2019) 052502.
[10] A. Spyrou, et al., Phys. Rev. Lett. 113 (2014) 232502.
[11] R. Santra, et al., Phys. Lett. B 806 (2020) 135487.
[12] G. Mantzouranis, H.A. Weidenmüller, D. Agassi, Z. Phys. A 276 (1976) 145–154.
[13] A.J. Koning, S. Hilaire, M.C. Duijvestijn, TALYS-1.0, in: Proceedings of the International Conference on Nuclear Data Science Technology 2007, EDP Science Nice, France, 2008, pp. 211–214.
[14] G. Potel, F.M. Nunes, I.J. Thompson, Phys. Rev. C 92 (2015) 034611.
[15] Jin Lei, Antonio M. Moro, Phys. Rev. C 97 (2018) 011601(R).
[16] C. Domingo-Pardo, C. Guerrero, F. Käppeler, C. Lederer, R. Reifarth, D. Schumann, J.L. Tain, Letter of Intent to the ISOLDE and Neutron Time-of-Flight Committee, 2014.
[17] A. Makinaga, R. Massarczyk, M. Beard, R. Schwengner, H. Otsu, T. Al-Abdullah, M. Anders, D. Bemmerer, R. Hannaske, R. John, A.R. Junghans, S.E. Müller, M. Röder, K. Schmidt, A. Wagner, Phys. Rev. C 94 (2016) 044304.
[18] S. Chiba, O. Iwamoto, Phys. Rev. C 81 (2010) 044604.
[19] J.E. Escher, F.S. Dietrich, Phys. Rev. C 81 (2010) 024612.
[20] E. Bauge, J.P. Delaroche, M. Girod, Phys. Rev. C 63 (2001) 024607.
[21] S. Michimasa, J.W. Hwang, K. Yamada, S. Ota, M. Dozono, N. Imai, et al., Prog. Theor. Exp. Phys. 043D01 (2019).
[22] T. Kubo, et al., Prog. Theor. Exp. Phys. 03C003 (2012).
[23] S. Michimasa, M. Takaki, M. Dozono, S. Go, H. Baba, E. Ideguchi, K. Kisamori, H. Matsubara, H. Miya, S. Ota, H. Sakai, S. Shimoura, A. Stolz, T.L. Tang, H. Tokieda, T. Uesaka, R.G.T. Zegers, Nucl. Instrum. Methods B 42 (2013) 710.
[24] S. Takeuchi, et al., RIKEN Accel. Prog. Rep. 49 (2016) 86.
[25] P.D. Kunz, https://www.oecd-nea.org/tools/abstract/detail/nesc9872.
[26] M. Dozono, T. Uesaka, S. Michimasa, M. Takaki, M. Kobayashi, M. Matsushita, S. Ota, H. Tokieda, S. Shimoura, Nucl. Instrum. Methods A 830 (2016) 233–242.
[27] A. Gilbert, A.G.W. Cameron, Can. J. Phys. 43 (1965) 1446.
[28] W. Dilg, W. Schantl, H. Vonach, M. Uhl, Nucl. Phys. A 217 (1973) 269.
[29] S. Kawada, M. Igashira, T. Katabuchi, M. Mizumoto, J. Nucl. Sci. Technol. 47 (2010) 643.
[30] A.J. Koning, D. Rochman, Nucl. Data Sheets 113 (2012) 2841.
[31] A.C. Kahler, et al., Nucl. Data Sheets 112 (2011) 2997–3036.
[32] K. Shibata, O. Iwamoto, T. Nakagawa, N. Iwamoto, A. Ichihara, S. Kunieda, S. Chiba, K. Furutaka, N. Otsuka, T. Ohsawa, T. Murata, H. Matsunobu, A. Zukeran, S. Kamada, J. Katakura, J. Nucl. Sci. Technol. 48 (1) (2011) 1–30.
[33] A. Di Pietro, K. Riisager, P. van Duppen, J. Phys. G, Nucl. Part. Phys. 44 (2017) 044013.